

Relativistic DFT Calculation of ^{119}Sn Chemical Shifts and Coupling Constants in Tin Compounds

Alessandro Bagno,^{*,†} Girolamo Casella,[‡] and Giacomo Saielli[§]

Dipartimento di Scienze Chimiche, Università di Padova, via Marzolo, 1-35131 Padova, Italy, Dipartimento di Chimica Inorganica e Analitica “Stanislao Cannizzaro”, Università di Palermo, Viale delle Scienze Parco d’Orleans II, 90128 Palermo, Italy, and Istituto CNR per la Tecnologia delle Membrane, Sezione di Padova, via Marzolo, 1-35131 Padova, Italy

Received July 18, 2005

Abstract: The nuclear shielding and spin–spin coupling constants of ^{119}Sn in stannane, tetramethylstannane, methyltin halides $\text{Me}_{4-n}\text{SnX}_n$ ($\text{X} = \text{Cl}, \text{Br}, \text{I}; n = 1–3$), tin halides, and some stannyl cations have been investigated computationally by DFT methods and Slater all-electron basis sets, including relativistic effects by means of the zeroth order regular approximation (ZORA) method up to spin–orbit coupling. Calculated ^{119}Sn chemical shifts generally correlate well with experimental values, except when several heavy halogen atoms, especially iodine, are bound to tin. In such cases, calculated chemical shifts are almost constant at the scalar (spin-free) ZORA level; only at the spin–orbit level is a good correlation, which holds for all compounds examined, attained. A remarkable “heavy-atom effect”, analogous to that observed for analogous alkyl halides, is evident. The chemical shift of the putative stannyl cation (SnH_3^+) has also been examined, and it is concluded that the spectrum of the species obtained in superacids is inconsistent with a simple SnH_3^+ structure; strong coordination to even weak nucleophiles such as FSO_3H leads to a very satisfactory agreement. On the contrary, the calculated ^{119}Sn chemical shift of the trimesitylstannyl cation is in very good agreement with the experimental value. Coupling constants between ^{119}Sn and halogen nuclei are also well-modeled in general (taking into account the large uncertainties in the experimental values); relativistic spin–orbit effects are again quite evident. Couplings to ^{13}C and ^1H also fall, on the average, on the same correlation line, but individual values show a significant deviation from the expected unit slope.

Introduction

The chemistry of tin compounds is important in a variety of contexts, spanning basic research and industrial applications.^{1–3} Tin exhibits two oxidation states, Sn(II) and Sn(IV), the latter being the more stable. Organometallic derivatives of Sn(IV) are produced in bulk amounts for a large variety of industrial,

agricultural, and biological uses.^{4,5} Their use in human cancer treatment is also documented.^{6,7}

Most of the structural properties of Sn(IV) compounds arise from its ability to expand its coordination number; this is often higher than the expected four, particularly when bound to more electronegative atoms or to weak donor ligands. This ability is responsible for differences between the solution phase and the solid-state structure of the same compound.

Although Mössbauer spectroscopy is a well-established technique for structure investigations of tin compounds in the solid state and frozen solutions, tin NMR is a more

* Corresponding author fax: +39 0498275239; e-mail: alessandro.bagno@unipd.it.

[†] Università di Padova.

[‡] Università di Palermo.

[§] Istituto CNR per la Tecnologia delle Membrane.

generally applicable tool to probe their structure and reactivity in solution. Natural tin occurs as three magnetically active isotopes: ^{115}Sn (natural abundance = 0.35%), ^{117}Sn (natural abundance = 7.61%), and ^{119}Sn (natural abundance = 8.58%).¹ Owing to their fairly high natural abundance, the ^{117}Sn and ^{119}Sn isotopes are amenable to experimental NMR studies, although ^{119}Sn is generally preferred, owing to its higher magnetogyric ratio. Very few usages of ^{115}Sn in NMR are reported.⁸

^{119}Sn chemical shifts cover a range from ca. +4000 to -2500 ppm, using tetramethyltin (SnMe_4) as a reference, and several reviews on tin NMR have been published.^{9–11} As is the case for most metal nuclei, there are few general rules to predict the relationship between structure and NMR spectral features. It is now established that several contributions affect ^{119}Sn chemical shifts, such as the nature of the ligands, the coordination number, the interaction with the solvent, the temperature, and the occurrence of self-association processes or inter-/intramolecular interactions. For example, for Sn(IV) , an approximate correlation between the ^{119}Sn chemical shift and its coordination environment is observed: increasing the coordination number causes an increased shielding. Therefore, from the value of the chemical shift, it is possible to estimate the coordination number.^{9–11} However, a relatively high correlation can only be observed for analogous compounds, for example, for organotin(IV) compounds with carbohydrate derivatives.^{12,13}

A survey about coupling constants between tin and several nuclei has been published, and the magnitude and sign of these couplings is often useful in structural investigations.¹⁴ When another nucleus is coupled to tin, normally both ^{119}Sn and ^{117}Sn satellite peaks are observed. $^1J(^{119}\text{Sn}, ^{13}\text{C})$ and $^2J(^{119}\text{Sn}, ^1\text{H})$ couplings obtained from the satellite signals are very useful in the structural determination of organotin(IV) compounds, and some empirical equations have been proposed to relate the spin–spin coupling constants to the C–Sn–C angle in dialkyltin(IV) derivatives.¹⁵ Moreover, a Karplus-like dependence of $^3J(^{119}\text{Sn}, ^2\text{H})$ has been observed.¹⁶

Other common Sn(IV) compounds, widely used in synthesis, are tin halides. For these, the direct measurement of $^1J(^{119}\text{Sn}, \text{X})$ ($\text{X} = \text{Cl}, \text{Br}, \text{I}$) is hampered by the fact that the extremely short T_1 of the quadrupolar halogen nuclei (generally $< 1 \mu\text{s}$) leads, at most, to a broadening of the tin NMR signal through scalar relaxation of the first kind. Thus, these direct spin–spin coupling constants have been derived by means of relaxation studies,^{17–19} although some direct measurements of $J(^{119}\text{Sn}, ^{35}\text{Cl})$ coupling constants in organotin chlorides have been reported.²⁰

The calculation of NMR properties by means of quantum-chemical methods is becoming an increasingly important tool in NMR spectroscopy. There is a substantial and growing data and knowledge base, indicating that, when suitable methods are adopted, all relevant molecular properties (nuclear shielding and spin–spin coupling constants) can be predicted with outstanding accuracy.^{21a} Like in the case of other nuclei, the theoretical study of chemical shifts and coupling constants of ^{119}Sn can usefully complement the structural analysis performed by means of experimental NMR data.

One of the issues associated with heavy-atom nuclei is the importance of relativistic effects thereon. Ziegler and co-workers have carried out a number of such pioneering investigations (of ^{183}W , ^{195}Pt , ^{199}Hg , ^{205}Tl , ^{207}Pb , and ^{235}U) and observed large relativistic effects on their NMR properties.^{21b,c} For lighter atoms such as Sn, these effects still have to be investigated in detail. For nuclei of similar atomic number such as Ru,²² Rh,²³ and Xe²⁴ and even higher such as W,²⁵ relativistic effects are intrinsically important (in that they affect nuclear shieldings) but often do not substantially affect the quality of calculated chemical shifts because the latter are the difference between the shieldings in two species, so that some contributions are almost constant and partly cancel. Thus, for example, an excellent agreement between experimental ^{99}Ru chemical shifts and nonrelativistic calculated values was obtained, even if that correlation included complexes where fairly heavy atoms (Sn and I) are bonded to Ru.²⁶ This cancellation of effects between reference and probe molecules may not hold when only one is subject to strong relativistic effects. This happens when one or more third- or fourth-row atoms (typically iodine) are bonded to an observed light nucleus and the bond has a high s character. In this case, spin–orbit (SO) coupling makes a large contribution to the overall shielding and generally causes the observed nucleus to be unusually shielded (see, e.g., ^{13}C in Cl_4 , $\delta = -290$ ppm). This effect has been related to a Fermi-contact mechanism intimately connected with the magnitude of the relevant coupling constant.²⁷

On the other hand, coupling constants involving heavy-atom nuclei have been found to be subject to large scalar relativistic effects even for moderately heavy nuclei such as those dealt with herein, and even more so for heavier nuclei.^{21b,c,28}

^{119}Sn NMR offers a unique environment to further test this situation since the reference compound (SnMe_4) only has light atoms, whereas there is a substantial data set pertaining to tin halides, comprising species where one or more halogen atoms from Cl to I are present. Some earlier theoretical investigations by Nakatsuji and co-workers considered $\text{Me}_n\text{SnH}_{4-n}$ and $\text{Me}_n\text{SnCl}_{4-n}$ at the self-consistent field level of theory,²⁹ later corrected by inclusion of SO coupling in the Hamiltonian, to account for the unusual shielding of tin when heavy atoms such as iodine are bound to it.³⁰ The origin of the SO effect was ascribed by the authors to the Fermi contact term. Semiempirical methods, such as a modified version of the AM1 model Hamiltonian,³¹ were also developed to study spin–spin coupling constants, including $^1J(\text{Sn}, \text{Sn})$.³² More recently, relativistic effects have been considered for simple systems such as SnH_4 and SnMe_4 ,^{33,34} but for larger organotin derivatives, nonrelativistic DFT methods have been used.^{35,36} Generally, a good agreement between theory and experiments has been found for chemical shifts.³⁷ In contrast, for spin–spin couplings, only highly correlated levels of theory, such as the complete active space self-consistent field^{38,39} or relativistic four-component methods,³⁴ have been able to quantitatively recover the measured $^1J(\text{Sn}, \text{H})$ and $^1J(\text{Sn}, \text{C})$ of SnH_4 and SnMe_4 . Therefore, it seems that the performance of DFT methods with respect to NMR properties of tin is not yet established

with sufficient generality, especially with regard to Sn compounds containing heavy atoms. It is, therefore, of interest to assess whether DFT is a valuable tool in quantitative predictions of ¹¹⁹Sn NMR properties, particularly spin–spin coupling constants involving it.

A further issue where these calculations may prove useful is connected to the isolation and spectroscopic studies of unstable tin species such as stannyl cations SnR_3^+ and anions SnR_3^- , SnH_3^+ and SnH_3^- being the respective parent compounds.

Computational Details

All calculations have been carried out using DFT as implemented in the Amsterdam density functional (ADF) code,⁴⁰ in which frozen-core, as well as all-electron, Slater basis sets are available for all atoms of interest. The ADF code also offers the possibility of taking relativistic effects into account, by means of the two-component zeroth-order regular approximation (ZORA) method,⁴¹ which requires specially optimized basis sets. With each method, it is possible to include either only scalar effects (the ZORA equivalents of Darwin and mass-velocity) or spin–orbit coupling as well.

Our previous works concerning Ru,²² Rh,²³ Xe,²⁴ and W²⁵ compounds, spanning a variety of bonding types and electronic structures, showed that the Becke 88 exchange⁴² plus the Perdew 86 correlation⁴³ (BP) functional performs rather well for the calculation of NMR properties, and this was also selected in this work. Moreover, in one case,²⁴ we also tested other functionals with no significant differences in the results. The all-electron TZ2P basis set (specially optimized for ZORA calculations) was used with all atoms. Relativistic frozen-core potentials (not to be confused with effective core potential basis sets), required to run relativistic calculations, were generated with the Dirac utility.⁴⁰ The geometries were optimized at the BP-ZORA/TZ2P level, taking full advantage of symmetry. All optimized geometries are reported as Supporting Information. Sn–H and Sn–C distances in SnH_4 and SnMe_4 were calculated to be 1.715 and 2.184 Å, respectively. The corresponding experimental values are 1.701 and 2.144 Å, respectively.⁴⁴ Using the larger QZ4P basis set for the optimization slightly improved the agreement for the Sn–C bond length of SnMe_4 (calcd 2.177 Å) but did not affect the Sn–H bond length of SnH_4 . As far as the tin–halogen bond distances are concerned, we have found an overestimation of similar magnitude, about 0.05 Å, compared to available experimental values.^{44f} Some data are reported as Supporting Information.

The ADF *nmr* property module then allows for the calculation of nuclear shieldings by either method.⁴⁵ Shieldings were then calculated at the BP-ZORA/TZ2P scalar and spin–orbit levels. These combinations will be denoted as SC and SO, respectively. In the former case, the isotropic shielding constant σ is given by the sum of diamagnetic and paramagnetic contributions ($\sigma = \sigma_d + \sigma_p$), whereas in the second one, the spin–orbit contribution is also added ($\sigma = \sigma_d + \sigma_p + \sigma_{\text{SO}}$). Computed chemical shifts are then determined by the difference of the shielding of the experimental standard SnMe_4 ($\delta = 0$) from $\delta = \sigma_{\text{ref}} - \sigma$.

Spin–spin coupling constants were calculated with the ADF *cpl* module,⁴⁶ with the BP functional and the ZORA method as above. In a nonrelativistic framework, Ramsey's theory⁴⁷ dissects the contributions to the coupling constant into the Fermi-contact (FC), diamagnetic spin–orbit (DSO), paramagnetic spin–orbit (PSO), and spin-dipole (SD) terms, so that the reduced coupling constant K is given by $K = K^{\text{FC}} + K^{\text{DSO}} + K^{\text{PSO}} + K^{\text{SD}}$. Within the ZORA approximation, the same terms can be calculated, although the FC, SD, and PSO terms contain cross terms with the others. Moreover, if a spin–orbit Hamiltonian is used, the individual FC and SD terms must be evaluated in two independent runs; in this work, we only report the total FC + SD term.

Results

¹¹⁹Sn Chemical Shifts in Alkyltin Halides. In organotin(IV) compounds, the solvent exerts a non-negligible influence on the chemical shift because, as mentioned before, it may strongly coordinate to the metal, thereby causing (among other things) a substantial geometry change. Therefore, to make a consistent comparison between experimental and calculated chemical shifts, we used experimental values acquired in noncoordinating solvents. Taking into account solvent effects would require at least the explicit inclusion of a few solvent molecules and long-range electrostatic contributions,⁴⁸ or even the consideration of the full dynamics of the solvated system, as recently done by Bühl et al. for some metal complexes.⁴⁹ This would render our computational protocol infeasible for the large set of compounds we have investigated. The experimental chemical shifts are reported in Table 1, together with the results of the calculations discussed below.

For tin halides (SnX_4) and methyltin halides ($\text{Me}_{4-n}\text{SnX}_n$; X = Cl, Br, I; $n = 1-3$), a strong “heavy-atom” effect is clearly evident: on the basis of the higher electronegativity of Br and I compared to that of C, one would have expected more and more deshielding of the Sn nucleus upon increasing the number of halogen atoms in the series $\text{Me}_{4-n}\text{SnX}_n$. In contrast, the observed trend is just the opposite, with a large upfield shift which increases strongly as methyl groups are replaced by halogens. This effect, fully analogous to that on ¹³C, was explained by Nakatsuji and co-workers³⁰ as originating from spin–orbit coupling in the Hamiltonian, a contribution that becomes more important for atoms of high atomic number. However, the authors did not perform a full relativistic calculation but limited their study to the inclusion of spin–orbit coupling within a Hartree–Fock approach. It is, therefore, of interest to extend such a study by means of a more-detailed relativistic calculation and larger basis set. Moreover, an “experimental” value of the shielding constant of the reference SnMe_4 has been reported as $\sigma(\text{SnMe}_4) = 2180 \pm 200$ ppm.⁵⁰ These data were estimated by means of the experimentally determined ¹¹⁹Sn spin-rotation constant combined with the calculated value of the shielding constant of the free tin atom. The latter calculation did not include relativistic effects.⁵¹ In Table 1, we report the results of our calculations at the two relativistic levels. We note that the scalar relativistic shielding of SnMe_4 is very close to the “experimental” value, while the result obtained at the spin–

Table 1. Experimental and Calculated ^{119}Sn Chemical Shifts (ppm)

species	ZORA scalar				ZORA spin-orbit					δ_{exptl}	ref
	σ_p	σ_d	σ	δ_{calcd}	σ_p	σ_d	σ_{so}	σ	δ_{calcd}		
SnMe_4	-2747	5030	2283	0	-2772	5032	489	2749	0	0	
$\text{Me}_3\text{SnSnMe}_3$	-2675	5032	2356	-73	-2700	5034	512	2845	-96	-113	52
SnH_4	-2148	5031	2883	-600	-2165	5033	513	3381	-632	-500 ^a	53
SnH_3^-	-1707	5032	3325	-1042	-1724	5034	511	3821	-1072		54
SnH_3^+	-3819	5028	1208	1074	-3847	5030	434	1617	1132	-186	55
$\text{SnH}_3^+\cdot\text{FSO}_3\text{H}^b$	-3017	5028	2011	272							
$\text{SnH}_3^+\cdot\text{FSO}_3\text{H}^c$	-2861	5028	2167	116							
$\text{SnH}_3^+\cdot 2\text{FSO}_3\text{H}^b$	-2821	5028	2207	76							
$\text{SnH}_3^+\cdot 2\text{FSO}_3\text{H}^c$	-2603	5028	2425	-142							
SnH_3F	-2577	5029	2452	-169							
$\text{Mes}_3\text{Sn}^{+d}$	-3589	5032	1443	840	-3624	5034	429	1839	910	806	56
Me_3SnCl	-2933	5031	2098	185	-2963	5034	493	2564	185	164	57
Me_2SnCl_2	-2952	5033	2080	203	-2986	5035	512	2561	188	141.2 ^e	58
MeSnCl_3	-2860	5034	2175	108	-2895	5036	565	2707	43	21	57
SnCl_4	-2731	5036	2306	-23	-2766	5038	687	2960	-210	-150	59
Me_3SnBr	-2945	5030	2085	198	-2975	5033	556	2614	136	128	57
Me_2SnBr_2	-3015	5030	2015	268	-3051	5033	696	2678	71	70	57
MeSnBr_3	-2981	5031	2050	233	-3022	5033	999	3010	-261	-165	60
SnBr_4	-2877	5031	2154	128	-2919	5034	1609	3723	-973	-638	59
Me_3SnI	-3146	5034	2085	198	-2977	5033	665	2721	28	39	57
Me_2SnI_2	-3086	5032	1946	337	-3132	5035	1037	2939	-190	-159	57
MeSnI_3	-3146	5034	1887	395	-3209	5036	1787	3614	-865	-700	61
SnI_4	-3109	5035	1927	356	-3174	5037	3079	4942	-2193	-1701	59
SnI_3Cl	-3024	5035	2012	271	-3080	5038	2527	4485	-1736	-1330, -1347	59
SnCl_3I	-2831	5036	2205	78	-2872	5038	1311	3477	-728	-543, -557	59

^a Extrapolated value. ^b F donor. ^c O donor. ^d Mes = 2,4,6-trimethylphenyl. ^e Saturated in CCl_4 .

orbit level is about 600 ppm larger, a deviation almost entirely due to the spin-orbit contribution (σ_{SO}) itself. It is worth noting that σ_{SO} is as large as 500 ppm, even for SnH_4 .

Concerning the scalar relativistic results, the diamagnetic contribution to the shielding constant (σ_d) is essentially constant (a 6-ppm variation) through the series, whereas the paramagnetic contribution (σ_p), spanning over 1000 ppm, is quite sensitive to the structure. However, these two contributions alone are not capable of reproducing, even qualitatively, the experimental trend. In fact, chemical shifts calculated at the scalar relativistic level are completely uncorrelated with the experimental values (see Figure 1). In contrast, the spin-orbit contribution is strongly dependent on the number and type of halogen atoms bound to tin; σ_{SO} amounts to 500–600 ppm if tin is coordinated to light atoms or chlorine, 600–1000 ppm for bromine, and 1000–3000 ppm for iodine. The chemical shifts calculated at the ZORA spin-orbit level (Figure 1) are in very good agreement with experimental data; therefore, almost all deviations calculated at the nonrelativistic³⁶ and scalar relativistic levels can be attributed to the missing σ_{SO} term.

It is worthwhile to discuss the difference between the calculated chemical shift at the scalar and spin-orbit levels in more detail. For the series $\text{Me}_{4-n}\text{SnX}_n$, upon increasing the number of halogen atoms (i.e., $n = 1, 2, 3, 4$), this difference respectively amounts to 0, 15, 65, and 187 ppm for $\text{X} = \text{Cl}$; 62, 197, 494, and 1101 ppm for $\text{X} = \text{Br}$; and 170, 527, 1260, and 2549 ppm for $\text{X} = \text{I}$. This trend highlights the importance of spin-orbit coupling when heavy atoms are bound to a central light atom, as already

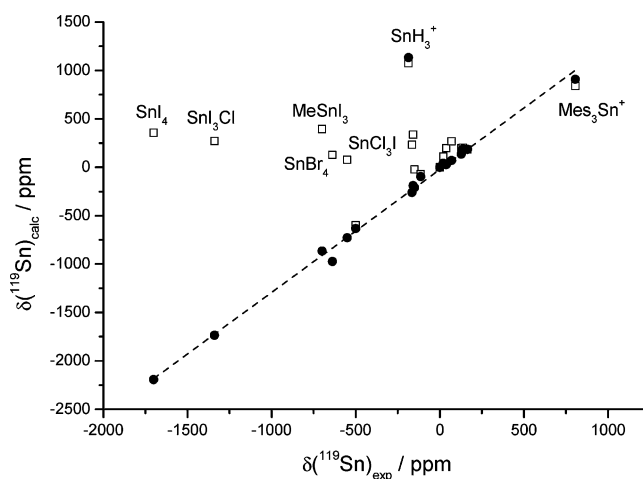


Figure 1. Correlation between calculated and experimental chemical shifts in tin compounds. BP-ZORA scalar (empty squares) and spin-orbit (filled circles), TZ2P basis set. $\delta_{\text{calc}} = a + b\delta_{\text{exp}}$, $a = -23.0$ ppm, $b = 1.27$; $r = 0.998$. The result for SnH_3^+ is not included in the fit (see text).

mentioned, and the nonadditivity of the effect. We note that even for chlorine such relativistic corrections are not negligible if the number of chlorine atoms is high. A similar, but smaller, effect was found for the ^{13}C nuclei of *o*-bromochlorobenzene.⁶²

Finally, we mention that the results of nonrelativistic calculations of ^{119}Sn chemical shifts (see the Supporting Information) are in very good agreement with those obtained at the relativistic ZORA-SC level. As already noted in the Introduction, when no other heavy atoms are directly bound

to the atom of interest, nonrelativistic levels of theory perform rather well for chemical shifts, even for metals. This finding should not obscure the fact that when other heavy atoms are present (as is the case for most species considered herein), relativistic effects must be considered.

¹¹⁹Sn Chemical Shift of Stannyl Cations. NMR has always been concerned with the structure elucidation of unstable species; indeed, the existence of carbocations has been proven by means of this technique. The awareness of this concept has spawned many studies in which the generation of the corresponding electron-deficient species based on Si, Ge, and Sn was attempted. However, despite their formal analogy with carbocations, their existence has been sharply debated, especially in the case of silyl (silicium) ions R_3Si^+ . There is now a general consensus that the stability of silicon, germanium, or tin cations is governed by profoundly different factors than carbocations and that these factors render them extremely electrophilic and incapable of existence as “free” or weakly solvated species in the same sense that is normally attributed to carbocations.⁶³ Nevertheless, under suitable conditions, silyl cations can be generated.⁶⁴

Quantum chemical calculations, especially of ²⁹Si NMR chemical shifts, have played a major role in establishing these conclusions. The level of accuracy that can currently be attained is such that one can rule out, or raise severe criticism against, structures that do not fit the theoretical expectations and provide indications as to what the actual structures should be. Thus, early experimental ²⁹Si NMR chemical shifts of putative silyl cations (ca. 110 ppm) were deemed too shielded in comparison with the expected values for an isolated silyl cation (ca. 350 ppm). However, it was also shown that coordination with a nucleophile as poor as an argon atom caused substantial shielding from the isolated-ion value, so that care must be taken to compare experimental data, obtained in condensed phases, with appropriate models.⁶³ As a further example, in our previous work dealing with xenon compounds, we pointed out that the ¹²⁹Xe spectrum of the species postulated as XeF^+ was inconsistent with that structure and that the bridged $Xe_2F_3^+$ cation would reconcile theoretical and experimental results.²⁴

It is then interesting to apply these notions to the case in point. An early attempt at generating a stannyl cation (SnH_3^+) in HSO_3F led to a ¹¹⁹Sn chemical shift of $\delta = -186$ ppm.⁵⁵ More recently, Lambert and co-workers reported on the generation of sterically hindered stannyl cations, and ¹¹⁹Sn chemical shifts ranging between 300 and 800 ppm were, thus, observed; in particular, the tris(2,4,6-trimethylphenyl)stannyl cation (Mes_3Sn^+) had $\delta = +806$ ppm.⁵⁶ More recently, Lambert was able to obtain the X-ray structure and NMR

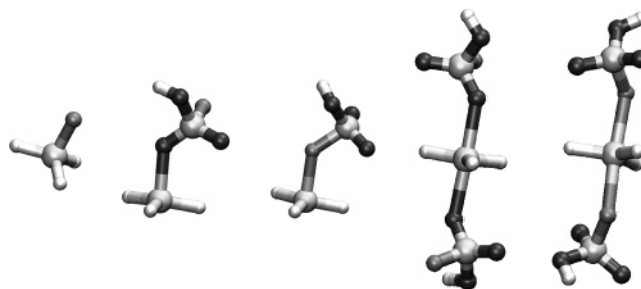


Figure 2. Optimized structures (ZORA scalar/TZ2P) of $SnH_3^+ \cdot X$ systems with $X = HSO_3F$, $2HSO_3F$, and F^- . From left to right: SnH_3F , $SnH_3^+ \cdot OSO(OH)F$, $SnH_3^+ \cdot FSO_2(OH)$, $SnH_3^+ \cdot 2OSO(OH)F$, and $SnH_3^+ \cdot 2FSO_2(OH)$.

spectrum of the tris(2,4,6-tri-isopropylphenyl)stannyl cation (Tip_3Sn^+) and provided a computed estimate of its ¹¹⁹Sn chemical shift of +763 ppm, to be compared with the experimental value of +716 ppm.⁶⁵

The remarkable agreement provides strong support for the concept that free stannyl ions can be generated in the solid state and in solution. On the other hand, by the same token, it is also evident that many experimental attempts have failed to provide such species. The prototypical example is given by the parent stannyl ion SnH_3^+ , for which the experimental⁵⁵ chemical shift is some 1300 ppm more shielded than the calculated value of ca. +1100 ppm (Table 1). Therefore, we have strived to provide computed estimates of the chemical shift of relevant stannyl cations in a consistent way and to understand the large variation in experimentally measured values.

The large disagreement indicates that the gas-phase structure of SnH_3^+ is not representative of the actual geometry. Therefore, we have optimized other structures that might have formed in the reaction medium, namely, $SnH_3^+ \cdot HSO_3F$ and $SnH_3^+ \cdot 2HSO_3F$, having oxygen or fluorine as donors, and SnH_3F , as in Figure 2. In Table 2, we report the relevant geometrical parameters.

The calculated ZORA scalar/TZ2P tin chemical shift is strongly influenced by coordination with other species, in full analogy with the behavior of silyl cations. Thus, even a nucleophile as weak as FSO_3H causes a major shielding of the tin nucleus: we obtain $\delta = +116$ ppm and $\delta = -142$ ppm for $SnH_3^+ \cdot HSO_3F$ and $SnH_3^+ \cdot 2HSO_3F$, respectively, with oxygen as the donor, and $\delta = +272$ ppm and $\delta = +76$ ppm for $SnH_3^+ \cdot HSO_3F$ and $SnH_3^+ \cdot 2HSO_3F$, respectively, with fluorine as the donor. Finally, the calculated shift of SnH_3F ($\delta = -169$ ppm), where any cationic character is lost, is in very good agreement with the experimental value of -186 ppm. This could be fortuitous since no evidence of such a compound was reported;⁵⁵ nevertheless, it is undeni-

Table 2. Some Geometrical Parameters of Species Related to SnH_3^+

	O donor			F donor		
	$r(Sn-O)/\text{\AA}$	$r(Sn-H)/\text{\AA}$	α/deg^a	$r(Sn-F)/\text{\AA}$	$r(Sn-H)/\text{\AA}$	α/deg^a
SnH_3^+		1.701	180		1.701	180
$SnH_3^+ \cdot HSO_3F$	2.247	1.699	167	2.240	1.697	162
$SnH_3^+ \cdot 2HSO_3F$	2.400	1.695	180	2.417	1.696	180
SnH_3F				1.956	1.714	133

^a Dihedral angle H–Sn–H–H, defining the out-of-plane bending of hydrogen atoms.

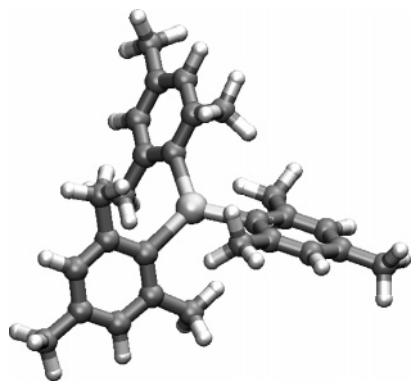


Figure 3. Optimized structure (ZORA scalar/TZ2P) of the tris-(2,4,6-trimethylphenyl)stannylum ion (Mes_3Sn^+).

able that the experimental chemical shift of SnH_3^+ actually pertains to a strongly solvated species; indeed, many compounds where tin is bonded to electron-withdrawing groups resonate in the same range.⁵⁶ The chemical shift of $\text{SnH}_3^+ \cdot 2\text{OSO}(\text{OH})\text{F}$ (Figure 2; $\delta = -142$ ppm) is indeed in good agreement with the observed value of -186 ppm. An analogous conclusion was reached by Cremer et al., who computationally investigated SnH_3^+ complexed with one and two water molecules.⁶⁶

On the other hand, the recently reported values⁵⁶ of $\delta = +700$ – 800 ppm for Tip_3Sn^+ and Mes_3Sn^+ agree with the calculated ones and are remarkably close to the value for the naked SnH_3^+ ion. To further probe the scope of ^{119}Sn NMR calculations in a consistent way, we have calculated the ^{119}Sn chemical shift of the trimesitylstannylum ion at the ZORA scalar and SO/TZ2P levels adopted herein. The optimized structure is shown in Figure 3 and features an almost planar coordination geometry of tin (Sn–C–C–C dihedral angle of only 5°).

The ortho methyl groups of the three mesityl substituents, located above and below the coordination plane, prevent tin from interacting with the solvent, in contrast to the case of SnH_3^+ . The calculated chemical shift of $+840$ ppm (Table 1) is, again, in very good agreement with the experimental value ($+806$ ppm) and is consistent with the tin atom being hardly coordinated to the solvent (benzene).

Spin–Spin Coupling Constants. Before discussing our results in detail, it is of interest to test the performance of the ZORA method in calculating the relativistic contribution to spin–spin coupling constants involving tin. A comparison can be made for the $^1J(^{119}\text{Sn}, ^1\text{H})$ of SnH_4 , for which a four-component random phase approximation approach gave a relativistic effect of about -700 Hz.³⁴ This method, however, does not properly treat electron correlation: a crude estimate made by the authors to include correlation effects reduced the relativistic contribution to about -550 Hz. The final result was still overestimated (in magnitude) by more than 100 Hz compared to the experimental value. The nonrelativistic value of $^1J(^{119}\text{Sn}, ^1\text{H})$ that we have obtained at the BP/TZ2P level (-1283 Hz) compared with our ZORA-SC (-1600 Hz) and ZORA-SO (-1550 Hz) results (Table 3) reveals a relativistic contribution of about -300 Hz, in fair agreement with the above proposal, considering the numerous approximations involved.

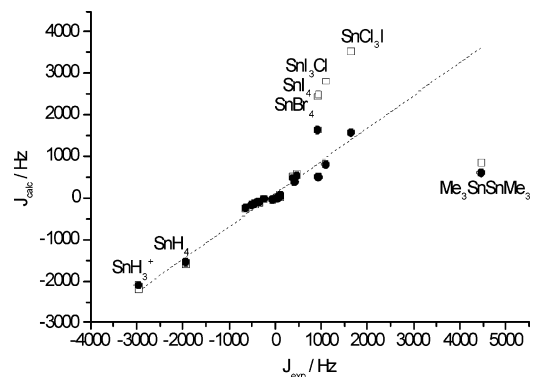


Figure 4. Correlation between calculated and experimental spin–spin coupling constants in tin compounds (ZORA scalar and SO/TZ2P). Scalar relativistic (empty squares) and spin–orbit relativistic (filled circles). $J_{\text{calc}} = a + bJ_{\text{exp}}$, $a = 101$ Hz, $b = 0.7898$; $r = 0.957$. The result for $\text{Me}_3\text{SnSnMe}_3$ is not included in the fit (see text).

One-bond tin–halogen coupling constants have been calculated for methyltin and tin halides. These coupling constants cannot be determined by recourse to splittings in the spectra, because the large nuclear quadrupole moments of Cl, Br, and I isotopes cause such signals to have exceedingly short relaxation times and correspondingly broad lines which are normally undetectable; as a consequence, they have been determined indirectly through their effect on the relaxation time of ^{119}Sn (scalar relaxation of the first kind).^{17–19} However, this procedure requires some assumption of the rotational correlation time, so there is some uncertainty associated with the experimental values. The coupling constants thus determined are reported in Table 3, together with the results of our calculations.

Spin–spin coupling between tin and chlorine has a non-negligible spin–orbit contribution which increases as the number of iodine atoms bonded to tin increases. In fact, the spin–orbit result improves the calculated $^1J(^{119}\text{Sn}, ^{35}\text{Cl})$, compared to the scalar calculation, by 6% in SnCl_4 , 9% in SnCl_3I , and 15% in SnI_3Cl . When we consider the couplings with the heavier atoms bromine and iodine, spin–orbit effects become essential in order to obtain a reasonable correlation, as we can see in Figure 4: $^1J(^{119}\text{Sn}, ^{127}\text{I})$ couplings in SnI_4 , SnI_3Cl , and SnCl_3I are all overestimated by some 2000 Hz (a factor of 2–4) compared to the spin–orbit calculation, the latter ones being in much better agreement with the experimentally estimated values (errors being 4–50%). The effect of the number of iodine atoms is, again, not additive. The calculated $^1J(^{119}\text{Sn}, ^{81}\text{Br})$ in SnBr_4 is overestimated, and in this case, the agreement with the experimentally derived data is not quantitative. We note, however, that an unusual dynamical behavior of SnBr_4 was reported,¹⁸ which might have affected the accuracy of the estimated coupling constant.

In all cases investigated here, the DSO contribution is negligible (10^{-1} Hz) and not reported in Table 3. In contrast, the PSO contribution is generally important, and it is strongly affected by the inclusion of spin–orbit coupling in the Hamiltonian.

For methyltin halides, we have also calculated the coupling constants with ^{13}C and ^1H . The results at the scalar and spin–orbit levels are listed in Table 3. These values are smaller

Table 3. Calculated and Experimental Coupling Constants Involving ¹¹⁹Sn (Hz) in Tin Compounds^a

species	X ^b	ZORA scalar			ZORA SO			J (exptl)	ref
		PSO	FC + SD	J (calcd)	PSO	FC + SD + Cross	J (calcd)		
SnMe ₄	C	13.15	-128.97	-115.93	13.70	-118.42	-104.83	-340	67
	H	1.73	6.59	8.45	1.77	4.84	6.74	53.9	68
Me ₃ SnSnMe ₃	Sn	-30.53	868.70	838.30	-174.02	775.54	601.66	4460	52
¹ J	C	12.65	-43.64	-31.16	12.98	-32.74	-19.92	-240	52
² J	H	1.91	1.11	2.97	1.94	-0.82	1.07	49	52
² J	C	0.37	-43.43	-42.99	-0.32	-41.20	-41.46	-56	52
³ J	H	-0.07	-16.04	-15.90	-0.14	-15.70	-15.63	-17.3	52
SnH ₄	H	4.74	-1604.34	-1599.63	4.68	-1554.11	-1549.47	(-)1930 ^c	69
SnH ₃ ⁺	H	19.09	-2207.85	-2188.67	19.12	-2112.89	-2093.68	(-)2960 ^d	55
SnH ₃ ⁻	H	-1.50	28.18	26.63	-2.90	84.14	81.19	109.4 ^e	54
Me ₃ SnCl	Cl	43.51	247.05	290.53	39.60	237.07	276.64	220 ^f	20
	C	18.69	-142.58	-124.02	19.38	-132.10	-112.85	-379.7	70
	H	2.28	3.92	6.29	2.35	2.11	4.54	58.2	71
Me ₂ SnCl ₂	Cl	71.77	309.44	381.18	64.64	299.67	364.28	220 ^f	20
	C	21.41	-194.14	-172.88	22.49	-184.73	-162.39	-468.4, -566	65,70
	H	2.29	4.62	6.94	2.40	2.86	5.28	68.2, 68.9	68,72
MeSnCl ₃	Cl	85.58	393.57	479.10	72.17	384.57	456.70		
	C	20.49	-330.70	-310.38	22.56	-322.90	-300.50		
	H	2.02	15.28	17.26	2.24	13.66	15.86	96.9	72
SnCl ₄	Cl	83.96	484.37	568.29	59.24	476.32	535.50	470	17
Me ₃ SnBr	Br	219.81	1036.12	1255.87	94.28	984.96	1079.18		
	C	18.77	-131.81	-113.20	19.09	-121.81	-102.88	-368.9, -380	67,70
	H	2.38	3.27	5.65	2.42	1.45	3.88	57.8	71
Me ₂ SnBr ₂	Br	380.86	1285.94	1666.69	171.95	1231.59	1403.43		
	C	21.63	-166.59	-145.16	21.40	-156.55	-135.35	-442.7	70
	H	2.50	2.23	4.56	2.61	0.29	2.65	66.7	70
MeSnBr ₃	Br	460.86	1624.97	2085.68	64.62	1577.79	1642.26		
	C	21.15	-269.16	-248.27	19.86	-255.96	-236.35	-640	67
	H	2.31	9.23	11.22	2.33	6.97	8.98		
SnBr ₄	Br	454.22	1988.92	2442.95	-334.65	1968.18	1633.34	920	18
Me ₃ SnI	I	217.35	1263.36	1480.67	-131.95	1225.32	1093.32		
	C	18.57	-117.08	-98.68	18.20	-106.43	-88.40		
	H	2.43	2.51	4.88	2.44	0.78	3.17		
Me ₂ SnI ₂	I	390.53	1510.12	1900.57	-210.70	1473.05	1262.27		
	C	21.71	-125.33	-103.85	19.17	-108.35	-89.42		
	H	2.67	-0.32	2.10	2.57	-2.48	-0.15		
MeSnI ₃	I	481.94	1779.49	2261.31	-648.94	1777.84	1128.78		
	C	22.33	-172.81	-150.76	16.08	-132.27	-116.49		
	H	2.59	0.71	2.84	2.27	-3.29	-1.47		
SnI ₄	I	488.65	2009.16	2497.64	-1597.98	2103.98	505.84	940	17
SnCl ₃ I	Cl	84.77	445.64	530.35	42.47	439.83	482.23	378 ^g	19
	I	483.80	3052.88	3536.61	-1606.86	3179.70	1572.76	1638	19
SnI ₃ Cl	Cl	86.08	369.64	455.62	22.96	363.27	386.14	421	19
	I	487.95	2321.11	2808.93	-1628.81	2434.83	805.89	1097	19

^a BP-ZORA scalar or SO/TZ2P. DSO terms are always negligible and are not reported. ^b X = ¹H, ¹³C, ³⁵Cl, ⁸¹Br, ¹¹⁹Sn, and ¹²⁷I. Coupling constants with ¹H in methyl groups are averaged assuming fast rotation. ^c Signs in parentheses have been inferred by comparison with similar molecules. ^d -78 °C. The sign has been assumed equal to the calculated one. ^e -78 °C. ^f Approximate value for triaryltin chlorides.²⁰ ^g Estimated using T₂ (³⁵Cl) for SnCl₄.

than with halogens and, therefore, occupy a small range in the plot of Figure 4. On the whole, they fall into the same correlation line of the other compounds. However, it is of interest to focus on this small region and discuss the behavior of this type of coupling because their magnitude is often related to the coordination pattern of tin; this is presented in Figure 5.

Unexpectedly, even though calculated carbon and proton coupling constants are well correlated with the experimental values, the slope of the linear fit (0.3) is far from unity. Since

these couplings are known to be very sensitive to the geometry of coordination around tin (and are commonly employed precisely for this purpose), to check for such an effect for the smaller systems (SnMe₄ and SnH₄), we have also repeated the calculation using the larger QZ4P basis set both for geometry optimization and for the calculation of the property. The results, however, were not significantly affected: calculated ¹J(¹¹⁹Sn, ¹³C) and ²J(¹¹⁹Sn, ¹H) in SnMe₄, at the higher level of theory, were -101.6 and +9.4 Hz, respectively, that is, rather similar to the results obtained with

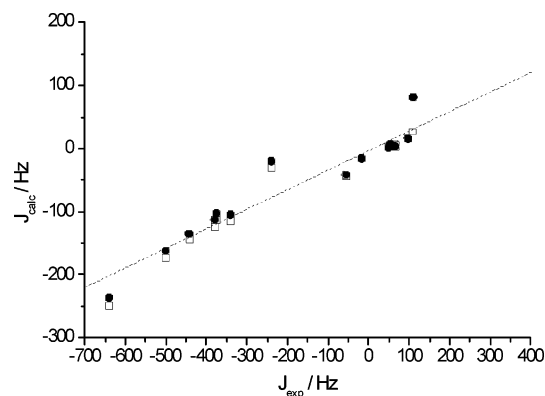


Figure 5. Correlation between calculated and experimental spin–spin coupling constants in tin compounds; expanded view on $J(^{119}\text{Sn}, ^1\text{H})$ and $J(^{119}\text{Sn}, ^{13}\text{C})$ coupling constants from the data of Figure 4. The fit line (dashed) $J_{\text{calc}} = a + bJ_{\text{exp}}$ has $a = -3.3$ Hz and $b = 0.309$; $r = 0.957$. Scalar relativistic (empty squares) and spin–orbit relativistic (filled circles).

the TZ2P basis set. On the other hand, calculation (TZ2P basis set) of the coupling constants using a SnMe_4 geometry with Sn–C bond lengths constrained to the experimental value yielded some improvement: -146.0 and $+9.9$ Hz for $J(^{119}\text{Sn}, ^{13}\text{C})$ and $J(^{119}\text{Sn}, ^1\text{H})$, respectively. A further test concerned Me_3SnBr , setting the Sn–Br distance to the experimental value^{44f} (see the Supporting Information) while the rest of the molecule was kept at the previously optimized BP/TZ2P geometry (in this case, the calculated Sn–C distance of 2.1713 Å was the same as the experimental value of 2.17 ± 5 Å). Again, some improvement was obtained for $J(^{119}\text{Sn}, ^{13}\text{C})$ and $J(^{119}\text{Sn}, ^1\text{H})$, being -120 and $+25$ Hz, respectively. However, such values remain quite far from the experimental results.

As a final test, we considered the performance of several GGA functionals. The results are fully reported as Supporting Information (Tables S4 and S5); herein, we will only report on the main conclusions. As we noted in our previous work on xenon compounds,²⁴ the performance of the various functionals is very similar: for example, $J(^{119}\text{Sn}, ^{13}\text{C})$ in SnMe_4 (ZORA scalar) ranges from a minimum of -107 Hz with the OPBE functional^{73a,73b} to a maximum of -132 Hz with the BLYP functional^{73c,73d} against an experimental value of -340 Hz. Therefore, even if BLYP appears to be somewhat superior, it underestimates the experimental result by more than 200 Hz. A slightly better result (-164 Hz at the ZORA scalar level), but still way off the experimental data, is obtained by using the BLYP functional in the calculation of the coupling constant together with the experimental geometry of SnMe_4 , as discussed above. The same considerations apply to the $J(^{119}\text{Sn}, ^1\text{H})$ value in SnMe_4 : the “best” calculated value (BLYP/experimental geometry; about $+10$ Hz) is less than 20% of the experimental coupling constant. It is presently unclear why the performance is worse than for other similar nuclei; however, such poor performance does not seem to be related to issues such as the choice of functional and basis set, or with geometry effects. We can only note that (a) other groups have reported similar inaccuracies with DFT methods^{33,39} and (b), more importantly, there are few if any other examples

where minute variations in coupling constants, arising from small structural changes, were investigated.

The only Sn–Sn coupling investigated herein pertains to hexamethylditin, $\text{Me}_3\text{SnSnMe}_3$. Whereas its calculated ^{119}Sn chemical shift is quite in line with the general level of accuracy attained, some of its coupling constants [most notably $J(^{119}\text{Sn}, ^{119}\text{Sn})$ but also $J(^{119}\text{Sn}, ^{13}\text{C})$] lie badly off the correlation line. In a pioneering study, experimental values were arrived at indirectly, through a detailed analysis of the ^1H and INDOR ^{119}Sn spectrum.⁵² Subsequent investigations confirmed the previous data and, at the same time, pointed out the extremely sensitive dependence of such couplings to even minute structural changes.⁷⁴ It then appears that ditin species still present a major challenge, in that subtle conformational, steric, and (possibly) solvent effects have to be considered.

We finally comment on the $J(^{119}\text{Sn}, ^1\text{H})$ values of SnH_3^+ and SnH_3^- . The former calculated value is some 30% off the experimental one, that is, with an error comparable to that of other compounds. Recalling the concerns expressed above on the nature of this species, this fair agreement is probably accidental, and we did not proceed with further evaluations. The value for SnH_3^- is also in rather good agreement with the calculated value. Since, however, no ^{119}Sn data were reported, it is difficult to judge whether the experimental conditions (deprotonation of SnH_4 with sodium in liquid ammonia) really led to SnH_3Na as claimed, although the high polarity of liquid NH_3 may indeed lead to an essentially “free” anion.⁵⁴

Conclusions

The calculation of ^{119}Sn chemical shifts and couplings by means of the ZORA relativistic method yields reliable results that may substantially aid in the structural elucidation of tin compounds. The wide array of species that can be studied includes some where heavy atoms such as iodine are bonded to tin; in such cases, we have shown relativistic spin–orbit corrections to be essential in order to provide a meaningful modeling. We have also shown how such calculations can identify incorrect assignments, like in the case of SnH_3^+ . The efficiency of the ADF code in handling these calculations should open the way to their widespread application in a broad range of structural and spectroscopic issues. However, when small variations in coupling constants are sought, like in the case of $J(^{119}\text{Sn}, ^1\text{H})$ and $J(^{119}\text{Sn}, ^{13}\text{C})$ in alkylstannanes, the performance is poorer despite an ample exploration of possible causes. Hence, there are still important issues to be addressed before such calculations enter into widespread usage.

Supporting Information Available: Cartesian coordinates of all structures optimized, experimental and calculated tin–halogen bond distances of methyltin halides and tin halides in the gas phase, nonrelativistic chemical shifts, and performance tests of various GGA functionals (14 pages). This material is available free of charge via the Internet at <http://pubs.acs.org>.

References

- (1) Davies, A. G. *Organotin Chemistry*; VCH: Weinheim, Germany, 1997.
- (2) Blunden, S. J.; Cusack, P. A.; Hill, R. *The Industrial Uses of Tin Chemicals*; The Royal Society of Chemistry: London, 1985.
- (3) *Chemistry of Tin*, 2nd ed.; Smith, P. J., Ed.; Blackie Academic & Professional: London, 1998.
- (4) Evans, C. J. In *Chemistry of Tin*, 2nd ed.; Smith, P. J., Ed.; Blackie Academic & Professional: London, 1998; Chapter 12, pp 442–479.
- (5) Arakawa, Y. In *Chemistry of Tin*, 2nd ed.; Smith, P. J., Ed.; Blackie Academic & Professional: London, 1998; Chapter 10, pp 388–428.
- (6) Saxena, A. K.; Huber, F. *Coord. Chem. Rev.* **1989**, *95*, 109–123.
- (7) Gielen, M. *Appl. Organomet. Chem.* **2002**, *16*, 481–494.
- (8) Meurice, J. C.; Vallier, M.; Ratier, M.; Duboudin, J. G.; Petraud, M. *J. Chem. Soc., Perkin Trans. 2* **1996**, 1311–1313.
- (9) Smith, P. J.; Tupčiauskas, A. P. *Annu. Rep. NMR Spectrosc.* **1978**, *8*, 291–370.
- (10) Wrackmeyer, B. *Annu. Rep. NMR Spectrosc.* **1985**, *16*, 73–186.
- (11) Wrackmeyer, B. *Annu. Rep. NMR Spectrosc.* **1999**, *38*, 203–264.
- (12) Grindley, T. B. *Adv. Carbohydr. Chem. Biochem.* **1998**, *53*, 17–142.
- (13) Pellerito, L.; Nagy, L. *Coord. Chem. Rev.* **2002**, *224*, 111–150 and references therein.
- (14) Wrackmeyer, B. In *Advanced Applications of NMR to Organometallic Chemistry*; Gielen, M., Willem, R., Wrackmeyer, B., Eds.; Wiley: Chichester, U. K., 1996; Chapter 4, pp 87–122.
- (15) (a) Lockhart, T. P.; Manders, W. F. *Inorg. Chem.* **1986**, *25*, 892–895. (b) Lockhart, T. P.; Manders, W. F. *J. Am. Chem. Soc.* **1987**, *109*, 7015–7020. (c) Holecěk, J.; Lyčka, A. *Inorg. Chim. Acta* **1986**, *118*, L15–L16. (d) Holecěk, J.; Nadvorník, M.; Handlir, K.; Lyčka, A. *J. Organomet. Chem.* **1986**, *315*, 299–308.
- (16) (a) Quintard, J. P.; Degueil-Castaing, M.; Dumartin, G.; Barbe, B.; Petraud, M. *J. Organomet. Chem.* **1982**, *234*, 27–40. (b) Quintard, J. P.; Degueil-Castaing, M.; Barbe, B.; Petraud, M. *J. Organomet. Chem.* **1982**, *234*, 41–61.
- (17) Sharp, R. R. *J. Chem. Phys.* **1972**, *57*, 5321–5330.
- (18) Sharp, R. R. *J. Chem. Phys.* **1974**, *60*, 1149–1157.
- (19) Sharp, R. R.; Tolan, J. W. *J. Chem. Phys.* **1976**, *65*, 522–530.
- (20) Apperley, D. C.; Haiping, B.; Harris, R. K. *Mol. Phys.* **1989**, *68*, 1277–1286.
- (21) (a) *Calculation of NMR and EPR Parameters*; Kaupp, M., Bühl, M., Malkin, V. G., Eds.; Wiley-VCH: Weinheim, Germany, 2004. (b) Autschbach, J. In *Calculation of NMR and EPR Parameters*; Kaupp, M., Bühl, M., Malkin, V. G., Eds.; Wiley-VCH: Weinheim, Germany, 2004; Chapter 14, pp 227–247. (c) Autschbach, J.; Ziegler, T. In *Calculation of NMR and EPR Parameters*; Kaupp, M., Bühl, M., Malkin, V. G., Eds.; Wiley-VCH: Weinheim, Germany, 2004; Chapter 15, pp 249–264.
- (22) Bagno, A.; Bonchio, M. *Magn. Reson. Chem.* **2004**, *42*, S79–S87.
- (23) Orian, L.; Bisello, A.; Santi, S.; Ceccon, A.; Saielli, G. *Chem.—Eur. J.* **2004**, *10*, 4029–4040.
- (24) Bagno, A.; Saielli, G. *Chem.—Eur. J.* **2003**, *9*, 1486–1495.
- (25) (a) Bagno, A.; Bonchio, M.; Sartorel, A.; Scorrano, G. *ChemPhysChem* **2003**, *4*, 517–519. (b) Bagno, A.; Bonchio, M. *Angew. Chem., Int. Ed.* **2005**, *44*, 2023–2025.
- (26) Bühl, M.; Gaemers, S.; Elsevier, C. J. *Chem. Eur. J.* **2000**, *6*, 3272–3280.
- (27) (a) Kaupp, M.; Malkina, O. L.; Malkin, V. G.; Pyykkö, P. *Chem. Eur. J.* **1998**, *4*, 118–126. (b) Kaupp, M.; Aubauer, C.; Engelhardt, G.; Klapötke, T. M.; Malkina, O. L. *J. Chem. Phys.* **1999**, *110*, 3897–3902.
- (28) Bryce, D. L.; Wasylishen, R. E.; Autschbach, J.; Ziegler, T. *J. Am. Chem. Soc.* **2002**, *124*, 4894–4900.
- (29) Nakatsuji, H.; Inoue, T.; Nakao, T. *J. Phys. Chem.* **1992**, *96*, 7953–7958.
- (30) Kaneko, H.; Hada, M.; Nakajima, T.; Nakatsuji, H. *Chem. Phys. Lett.* **1996**, *261*, 1–6.
- (31) Dewar, M. J. S.; Zebisch, E. G.; Healy, E. F.; Stewart, J. J. P. *J. Am. Chem. Soc.* **1985**, *107*, 3902–3909.
- (32) (a) Aucar, G. A.; Botek, E.; Gómez, S.; Sproviero, E.; Contreras, R. H. *J. Organomet. Chem.* **1996**, *524*, 1–7. (b) González, J. A.; Aucar, G. A.; Ruiz de Azúa, M. C.; Contreras, R. H. *Int. J. Quantum Chem.* **1997**, *61*, 823–833.
- (33) Khandogin, J.; Ziegler, T. *J. Phys. Chem. A* **2000**, *104*, 113–120.
- (34) Enevoldsen, T.; Visscher, L.; Saue, T.; Jensen, H. J. A.; Oddershede, J. *J. Chem. Phys.* **2000**, *112*, 3493–3498.
- (35) Avalu, P.; Harris, R. K.; Karadakov, P. B.; Wilson, P. J. *Phys. Chem. Chem. Phys.* **2002**, *4*, 5925–5932.
- (36) Vivas-Reyes, R.; De Proft, F.; Biesemans, M.; Willem, R.; Geerlings, P. *J. Phys. Chem. A* **2002**, *106*, 2753–2759.
- (37) de Dios, A. C. *Magn. Reson. Chem.* **1996**, *34*, 773–776.
- (38) Kirpekar, S.; Jensen, H. J. A.; Oddershede, J. *Chem. Phys.* **1994**, *188*, 171–181.
- (39) Malkina, O. L.; Salahub, D. R.; Malkin, V. G. *J. Chem. Phys.* **1996**, *105*, 8793–8800.
- (40) te Velde, G.; Bickelhaupt, F. M.; Baerends, E. J.; Fonseca Guerra, C.; van Gisbergen, S. J. A.; Snijders, J. G.; Ziegler, T. *J. Comput. Chem.* **2001**, *22*, 931–967. See also: <http://www.scm.com>.
- (41) Jensen, F. *Introduction to Computational Chemistry*; Wiley: Chichester, U. K., 1999; p 204.
- (42) Becke, A. D. *Phys. Rev. A* **1988**, *38*, 3098–3100.
- (43) Perdew, J. P. *Phys. Rev. B* **1986**, *33*, 8822–8824.
- (44) (a) Vilkov, L. V.; Mastryukov, V. S.; Sadova, N. I. *Determination of the Geometrical Structure of Free Molecules*; Mir Publisher: Moscow, 1983. (b) Wilkinson, G. R.; Wilson, M. K. *J. Chem. Phys.* **1956**, *25*, 784–784. (c) Beagley, B.; McAloon, K.; Freeman, J. M. *Acta Crystallogr. B* **1974**, *30*, 444–449. (d) Clark, H. C.; Furnival, S. G.;

- Kwon, J. T. *Can. J. Chem.* **1963**, *41*, 2889–2897. (e) Fujii, H.; Kimura, M. *Bull. Chem. Soc. Jpn.* **1970**, *44*, 2643–2647. (f) Zubietta, J. A.; Zuckerman, J. J. *Prog. Inorg. Chem.* **1978**, *24*, 251–475.
- (45) (a) Schreckenbach, G.; Ziegler, T. *J. Phys. Chem.* **1995**, *99*, 606–611. (b) Schreckenbach, G.; Ziegler, T. *Int. J. Quantum Chem.* **1997**, *61*, 899–918. (c) Wolff, S. K.; Ziegler, T. *J. Chem. Phys.* **1998**, *109*, 895–905. (d) Wolff, S. K.; Ziegler, T.; van Lenthe, E.; Baerends, E. J. *J. Chem. Phys.* **1999**, *110*, 7689–7698.
- (46) (a) Autschbach, J.; Ziegler, T. *J. Chem. Phys.* **2000**, *113*, 936–947. (b) Autschbach, J.; Ziegler, T. *J. Chem. Phys.* **2000**, *113*, 9410–9418.
- (47) Ramsey, N. F. *Phys. Rev.* **1953**, *91*, 303–307.
- (48) Autschbach, J.; Le Guennic, B. *Chem.—Eur. J.* **2004**, *10*, 2581–2589.
- (49) (a) Bühl, M.; Mauschick, F. T.; Terstegen, F.; Wrackmeyer, B. *Angew. Chem., Int. Ed.* **2002**, *41*, 2312–2315. (b) Bühl, M.; Mauschick, F. T. *Phys. Chem. Chem. Phys.* **2002**, *4*, 5508–5514. (c) Grigoleit, S.; Bühl, M. *Chem.—Eur. J.* **2004**, *10*, 5541–5552. (b) Bühl, M.; Schurhammer, R.; Imhof, P. *J. Am. Chem. Soc.* **2004**, *126*, 3310–3320.
- (50) Laaksonen, A.; Wasylishen, R. E. *J. Am. Chem. Soc.* **1995**, *117*, 392–400.
- (51) Malli, G.; Froese, C. *Int. J. Quantum Chem. Symp.* **1967**, *1*, 95–98.
- (52) McFarlane, W. *J. Chem. Soc. A* **1968**, 1630–1634.
- (53) Mitchell, T. N.; Amamria, A.; Fabisch, B.; Kuivila, H. G.; Karol, T. J.; Swami, K. *J. Organomet. Chem.* **1983**, *259*, 157–164.
- (54) Birchall, T.; Pereira, A. *J. Chem. Soc., Chem. Commun.* **1972**, 1150–1151.
- (55) Webster, J. R.; Jolly, W. L. *Inorg. Chem.* **1971**, *10*, 877–879.
- (56) Lambert, J. B.; Zhao, Y.; Wu, H. W.; Tse, W. C.; Kuhlmann, B. *J. Am. Chem. Soc.* **1999**, *121*, 5001–5008.
- (57) van den Berghe, E. V.; van der Kelen, G. P. *J. Organomet. Chem.* **1971**, *26*, 207–213.
- (58) Lassigne, C. R.; Wells, E. J. *Can. J. Chem.* **1977**, *55*, 927–931.
- (59) Burke, J. J.; Lauterbur, P. C. *J. Am. Chem. Soc.* **1961**, *83*, 326–331.
- (60) McFarlane, W.; Wood, R. J. *J. Organomet. Chem.* **1972**, *40*, C17–C20.
- (61) Kennedy, J. D.; McFarlane, W.; Pyne, G. S.; Clarke, P. L.; Wardell, J. L. *J. Chem. Soc., Perkin Trans. 2* **1975**, 1234–1239.
- (62) Bagno, A.; Rastrelli, F.; Saielli, G. *J. Phys. Chem. A* **2003**, *107*, 9964–9973.
- (63) Reed, C. A. *Acc. Chem. Res.* **1998**, *31*, 325–332.
- (64) Kim, K. C.; Reed, C. A.; Elliott, D. W.; Müller, L. J.; Tham, F.; Lin, L. J.; Lambert, J. B. *Science* **2002**, *297*, 825–827.
- (65) Lambert, J. B.; Lin, L.; Keinan, S.; Müller, T. *J. Am. Chem. Soc.* **2003**, *125*, 6022–6023.
- (66) Cremer, D.; Olsson, L.; Reichel, F.; Kraka, E. *Isr. J. Chem.* **1993**, *33*, 369–385.
- (67) McFarlane, W. *J. Chem. Soc. A* **1967**, 528–530.
- (68) Flitcroft, N.; Kaesz, H. D. *J. Am. Chem. Soc.* **1963**, *85*, 1377–1380.
- (69) Schumann, C.; Dreeskamp, H. *J. Magn. Reson.* **1970**, *3*, 204–217.
- (70) Petrosyan, V. S.; Pernin, A. B.; Reutov, O. A.; Roberts, J. D. *J. Magn. Reson.* **1980**, *40*, 511–518.
- (71) Petrosyan, V. S. *Prog. NMR Spectrosc.* **1977**, *11*, 115–148.
- (72) Kuivila, H. G.; Kennedy, J. D.; Tien, R. Y.; Tyminski, I. J.; Pelczar, F. L.; Khan, O. R. *J. Org. Chem.* **1971**, *36*, 2083–2088.
- (73) (a) Handy, N. C.; Cohen, A. J. *Mol. Phys.* **2001**, *99*, 403–412. (b) Perdew, J. P.; Burke, K.; Ernzerhof, M. *Phys. Rev. Lett.* **1996**, *77*, 3865–3868. (c) Becke, A. D. *Phys. Rev. A* **1988**, *38*, 3098–3100. (d) Lee, C.; Yang, W.; Parr, R. G. *Phys. Rev. B* **1988**, *37*, 785–789.
- (74) (a) Mitchell, T. N. *J. Organomet. Chem.* **1974**, *70*, C1–C2. (b) Harris, R. K.; Mitchell, T. N.; Nesbitt, G. J. *Magn. Reson. Chem.* **1985**, *23*, 1080–1081.

CT050173K